Effects of block copolymer self-assembly on optical anisotropy in azobenzene-containing PS-*b*-PMMA films

2012 Nanotechnology 23 115604

(http://iopscience.iop.org/0957-4484/23/11/115604)

IOP PUBLISHING NANOTECHNOLOGY
Nanotechnology **23** (2012) 115604 (8pp) doi:10.1088/0957-4484/23/11/115604

Effects of block copolymer self-assembly on optical anisotropy in azobenzene-containing PS-*b*-PMMA films

A B Orofino, M F Camezzana, M J Galante, P A Oyanguren and I A Zucchi

Institute of Materials Science and Technology (INTEMA), University of Mar del Plata and National Research Council (CONICET), J B Justo 4302, 7600 Mar del Plata, Argentina

E-mail: ileanazu@yahoo.com.ar

Received 15 November 2011, in final form 12 January 2012
Published 28 February 2012
Online at stacks.iop.org/Nano/23/115604

Abstract
Polystyrene-*b*-polymethylmethacrylate (PS-*b*-PMMA) was selected as the host for 4-(4-nitrophenylazo)aniline (Disperse Orange 3, DO3) based on a previous study of DO3/PMMA and DO3/PS binary blends. Selective location of DO3 into the PMMA block of the copolymer was expected during self-assembly of the block copolymer since a preferential interaction of DO3 with PMMA has been demonstrated. However, surface segregation of DO3 was found during the thermal annealing used to nanostructure the copolymer. To avoid this, a thermoplastic polymer (Azo-TP) was synthesized from the bulk reaction of DO3 and diglycidyl ether of bisphenol A (DGEBA). The choice of DGEBA as a co-reactant was an attempt to encourage the selective location of azo groups in the PMMA phase of PS-*b*-PMMA. An inspection of solutions of Azo-TP in PS and PMMA, corroborates the preferential affinity of Azo-TP for PMMA. The Azo-TP could be satisfactorily dissolved in PS-*b*-PMMA. We have investigated the growth and decay processes of the optically induced birefringence in films of PS-*b*-PMMA containing 12 wt% Azo-TP. The resulting materials showed a good photoinduced time response, high maximum birefringence and an elevated fraction of remnant anisotropy.

(Some figures may appear in colour only in the online journal)

1. Introduction

An exciting development in modern technology is the possibility of using light, instead of electric fields, to control the behavior of photonic components in highly integrated optical communication systems. The current rapid development of high-data-rate, fiber-optic communication and real-time information processing systems has created a need for all-optical, ultrahigh-speed photonic switches, which would eliminate the need to convert photonic signals into electrical ones, and vice versa. Light-responsive materials react to external stimuli with changes in their mechanical, electrical and optical properties [1]. In this framework, polymers containing azobenzene chromophores are among the most promising materials for photo-switchable devices, since azobenzene derivates undergo reversible *trans–cis* isomerization processes upon illumination with light (photoisomerization), providing a mechanism for chromophore photo-orientation [2]. The photo-orientation is achieved by excitation of the azobenzene chromophores with linearly polarized light, which leads to successive isomerization and reorientation of the chromophores with a sufficiently large transition dipole moment along the direction of the exciting field. The molecules tend to line up perpendicular to the polarization direction of the excitation beam, thus becoming inert to the incident irradiation. The anisotropic orientation of the chromophores leads to in-plane birefringence, which can be nondestructively read with a nonresonant probe beam and erased by randomizing the molecular orientation with, for example, circularly polarized

light. Once the excitation light has been turned off, the birefringence decreases because of thermal diffusion and *cis–trans* isomerization of the chromophores. Both the fraction of remnant birefringence and the efficiency of photo-orientation are the main properties that define the quality of the obtained material and are highly dependent on the structure of the chromophores as well as on their local environment [3].

A facile and easy-to-process method to obtain these materials is provided by guest–host polymers where the chromophores are simply mixed into a polymer matrix. These systems are simple and cost-effective, as they only require mixing of the constituents in order to produce the desired compound. However, their performance is limited by chromophore aggregation and phase separation, resulting in increased optical scattering losses, lowered optical response and poor temporal stability [4, 5].

To overcome the problems of guest–host systems, the active molecules have been covalently linked to the polymer backbone as either a pendant group or a co-monomer [6–8]. Such covalently functionalized polymers can have a large response to optical fields. Moreover, the induced anisotropy in such systems can be highly stable. Recently, the development of block copolymers (BC) covalently functionalized with azobenzene units has gained importance, since the confinement of photo-responsive units in nanosized block copolymer domains gives these materials unique properties. BC nanostructuration eliminated the scattering of visible light [9, 10] and at the same time reduced azo aggregation [11, 12]. However, covalently linked systems in general, and BC in particular, are less attractive than guest–host systems, because complicated organic synthesis is required for each combination of a polymer and an active molecule.

In this paper we propose an alternative method to obtain azo-containing diblock copolymers (DBC) that combines the advantages of a guest–host system (like easy processability) with the unique properties of BC. We selectively introduce an azo dye into one block of the DBC by working on preferential interactions (or affinities). The resulting system showed no scattering of visible light and improved optical properties with respect to the simple guest–host system.

2. Experimental section

2.1. Materials

The chemical structures of the different compounds are shown in figure 1. A push–pull azo dye, 4-(4-nitrophenylazo)aniline (Disperse Orange 3, DO3, Aldrich; T_m = 200 °C), was selected as the photosensitive molecule. An azo-containing thermoplastic (Azo-TP) was synthesized from the bulk reaction of DO3 and diglycidyl ether of bisphenol A (DGEBA, DER332) in an amine/epoxy ratio equal to 0.5 [13]. The commercial asymmetric DBC polystyrene-*b*-polymethylmethacrylate (PS-*b*-PMMA), with a volume fraction of PMMA block equal to 0.29 (Mn = 67 100, PDI = 1.09), PS (Mn = 45 000, PDI = 1.05) and PMMA (Mn = 21 500, PDI = 1.4), were all purchased from Polymer Source Inc and used without further purification.

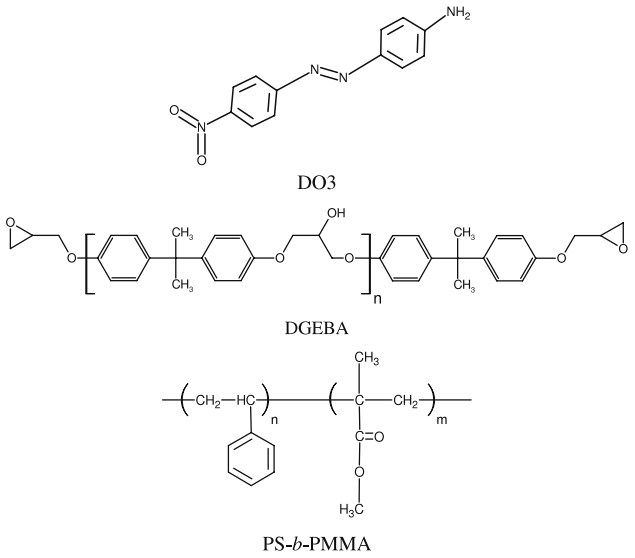

Figure 1. Chemical structures of DO3, DGEBA and PS-*b*-PMMA.

2.2. Film deposition

Tetrahydrofuran (THF) solutions of the cited DBC or one of their constitutive homopolymers (PS or PMMA) and the azo component were spin-coated at 3000 rpm onto previously cleaned Si or glass wafers. Film thicknesses in the range of 100–300 nm were obtained by changing the solution concentration. To promote self-assembly of the DBC the films were heated at 190 °C for 1 h.

2.3. Characterization

The morphology of the polymeric films was characterized by scanning electron microscopy (Zeiss Supra 40 SEM with a field emission source), operated at an acceleration voltage of 5 keV and using a secondary-electron detector (InLens).

Photoinduced birefringence of the resulting films was determined using the experimental set-up described in figure 2. Birefringence was measured by placing the sample between two crossed linear polarizers. A semiconductor laser at 488 nm (Coherent Sapphire^{TM} 488-20 OEM Laser Optically Pumped Semiconductor Laser) was used as a writing beam to induce optical anisotropy in the polymer film, and another semiconductor laser at 635 nm (laser diode, model I-R-5-P) was used as a reading beam to measure the power that is transmitted through this optical setup. To achieve the maximum signal, the polarization vector of the writing beam was set to 45° with respect to the polarization vector of the reading beam. All measurements were performed at room temperature and all the films were irradiated with 20 mW mm^{-2} of the writing laser. The change in the transmission of the reading beam, which passed through the sample between two crossed polarizers, was measured with a photodiode. The induced optical birefringence (Δn) was

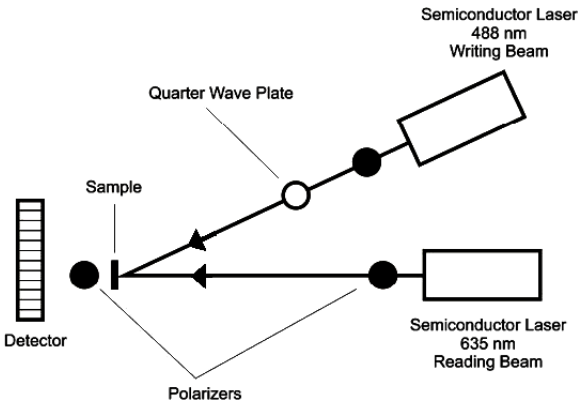

Figure 2. Schematic illustration of the experimental set-up for the measurement of the photoinduced orientation of azo compounds.

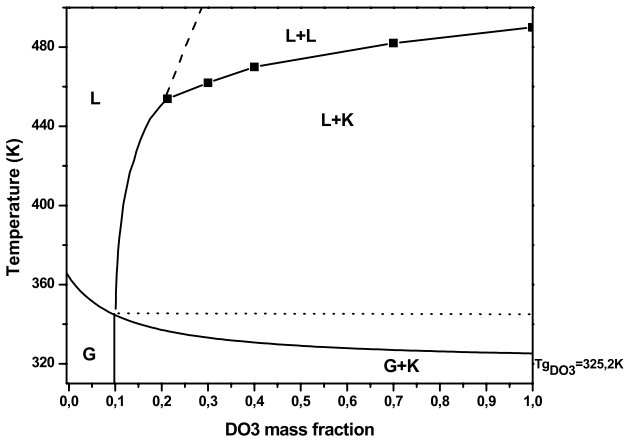

Figure 3. Phase diagram of DO3/PMMA blend.

determined by measuring the reading beam transmission ($T = I/I_0$) using

$$\Delta n = (\lambda/\pi d)\sin^{-1}(I/I_0)^{1/2} \quad (1)$$

where λ is the wavelength of the reading beam, d is film thickness, I is the intensity of the reading beam after the second polarizer and I_0 is the transmitted intensity of the reading beam between parallel polarizers in absence of anisotropy. In order to erase the photoinduced birefringence, a removable quarter-wave plate was used to induce circular polarization in the argon laser (erasing beam).

Differential scanning calorimetry (DSC) was performed using a Pyris 1 device (PerkinElmer). From the thermograms obtained in heating scans at 10 °C min^{-1} the following parameters were determined: glass transition temperature (T_g) defined at the onset of the change in specific heat and melting temperature (T_m) defined at the end of the melting peak.

UV–vis spectra were recorded with an Agilent 8453 diode array spectrophotometer. Glass-supported films were directly irradiated and spectra recorded at room temperature.

Near-infrared spectroscopy (NIR) was used to follow the conversion of epoxy groups in the reaction of DGEBA and DO3 at 180 °C. A FTIR device (Nicolet 6700 FTIR), provided with a heated transmission cell (HT-32 Spectra Tech) and a programmable temperature controller (Omega, Spectra Tech, $\Delta T = \pm 1$ °C), was employed. The initial formulation was placed between two glass covers separated by about 2 mm. The height of the epoxy absorption peak at 4530 cm^{-1} was followed as a function of reaction time.

The thickness of the films was evaluated by atomic force microscopy (AFM) imaging operating in contact mode (Agilent Technologies, 5500 scanning probe microscope). The film was scratched with a needle, and the height difference between the bare substrate surface and the film surface was estimated.

Transmission optical microscopy (TOM) was employed to determine the solubility limit of azo compounds in different solutions using a Leica DMLB microscope equipped with a hot stage (Linkam THMS 600).

3. Results and discussion

DO3 was selected since it is a push–pull dye and consequently it could be oriented to produce an anisotropic material using only one wavelength writing laser. At the same time, it has another important advantage, namely the primary amine present in its structure. This reactive group will allow us to eventually manage its affinity towards a matrix through a chemical reaction with epoxy.

A guest–host system consisting of DO3 dispersed in PMMA was first tested just in order to measure the solubility of DO3 in PMMA, since it is well known that this kind of film shows poor optical properties.

A phase diagram of the DO3/PMMA binary blend was needed to analyze their mutual solubility. The phase diagram of figure 3 was built up from the melting and devitrification temperatures of different solutions of DO3 in PMMA. One-phase regions (liquid (L) or glass (G)) and two-phase regions (liquid (L) + crystal (K), glass (G) + crystal (K) and liquid (L) + liquid (L)) are present in the phase diagram. The crystalline phase corresponded to pure DO3 crystals.

As we can appreciate in figure 3, blends containing up to 10 wt% of DO3 were homogeneous. In this range of compositions, DO3 acts as a plasticizer of PMMA and in consequence only one thermal transition corresponding to the glass transition of the homogeneous blend was present. For DO3 contents in the range between 10 and 30 wt%, crystallization was too slow during cooling, generating a metastable homogeneous glass, then crystallization took place during heating leading to the melting temperatures of the diagram.

In blends with concentrations above 30 wt% of DO3, crystallization was accelerated and occurred during cooling from the L–L state. Vitrification of a liquid phase containing 10 wt% DO3 and crystallization of the excess of DO3 occurred when cooling below 345 K. A heating scan of these samples showed, first, the devitrification of the phase containing 10 wt% of DO3 followed by the melting of the crystals of DO3 corresponding to the separated phase. As melting proceeded, the liquid phase changed its composition

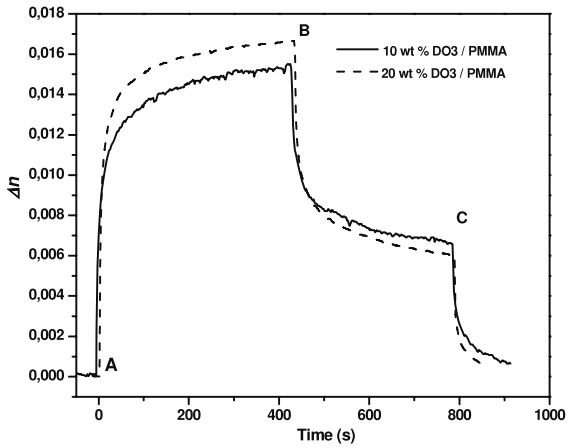

Figure 4. Writing and erasing curve of PMMA films containing 10 and 20 wt% DO3.

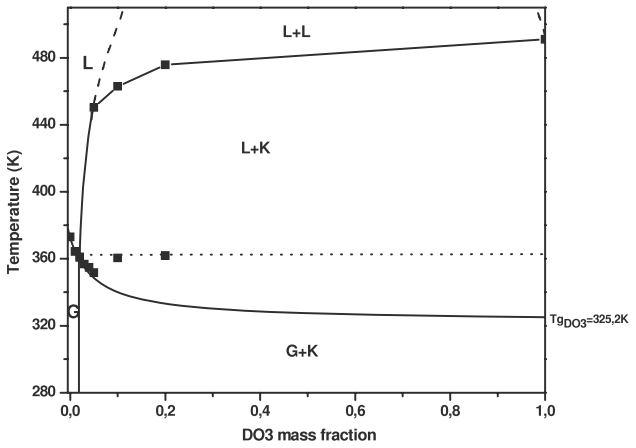

Figure 5. Phase diagram of DO3/PS blend.

following the curve that divided the liquid and crystalline regions to finally arrive at its initial composition, when the system became one or two liquid phases.

The solubility limit of DO3 in PMMA found by DSC was cross-checked by SEM. Samples containing up to 10 wt% DO3 were completely homogeneous, but blends exceeding this limit showed phase separated crystalline domains of DO3 dispersed in a continuous PMMA rich phase.

We have investigated the growth and decay processes of the optically induced birefringence in films of PMMA containing different amounts of DO3. Optical anisotropy in polymeric films results from the reorientation of the azobenzene moieties. Generally, linearly polarized light is used to photoinduce birefringence through *trans–cis–trans* isomerization cycles of azobenzene molecules. The absorption and reorientation sequence will be repeated until the dipole moment of azobenzene molecules lies in a direction which is perpendicular to the polarization direction of the writing beam. In this way, optical anisotropy can be induced in the films. In figure 4 writing–relaxing sequences obtained for PMMA films modified with 10 and 20 wt% of DO3 are plotted. In both cases, the reading beam continuously illuminates the samples.

At the beginning of the experiment there is no transmission of the reading beam, as the azo-chromophores in *trans* form, which is the more stable configuration, are randomly distributed. The films are isotropic. When the writing beam was turned on (point A), the reading beam was transmitted through the 'polarizer–sample–polarizer' system due to the optical anisotropy induced in the films. Photoinduced birefringence rapidly built up to the saturation level. When the excitation light is turned off (at point B), the signal starts to drop to a relaxed level where the rate of change of anisotropy is very small. The fraction of the saturation signal remaining at point C is called 'remnant birefringence'. To remove the remaining birefringence, circularly polarized light is introduced at point C.

As expected, $\Delta n_{\max}$ is proportional to the azo content, being higher for the sample with 20 wt% of DO3. When the writing laser is switched off there is an extreme relaxation process which leaves no more than 42 and 35% (corresponding to 10 and 20 wt% DO3, respectively) of the saturation signal in about 6 min. The big loss of anisotropic ordering is due to the facility of DO3-free molecules to move and is more accentuated in the sample where DO3 is aggregated (20 wt%).

It is postulated that the loss of anisotropic ordering could be suppressed by a confinement effect. In consequence, it would be interesting to know how azobenzene molecules behave in a confined geometry with reference to the photoalignment properties. Such a confining environment may be provided by self-organized nanodomains in DBC. If the guest is confined within a specific domain of a microstructured DBC due to immiscibility in the surrounding block component, the microstructure may further frustrate any reorientation and aggregation of the chromophore.

Since a relatively high solubility of DO3 in PMMA has already been proven, the selected DBC was the well-known PS-*b*-PMMA, hypothesizing that the solubility of DO3 in PS should be much lower in comparison. Indeed, to confirm this fact the following step was to measure the solubility limit of DO3 in PS.

A phase diagram of the DO3/PS binary blend similar to that measured for DO3/PMMA was built up from the melting and devitrification temperatures of different solutions of DO3 in PS, figure 5.

In the phase diagrams of figures 3 and 5 the curve that divides the liquid (L) and glass (G) zones represents the variation of T_g with the composition of the homogeneous blend. Both curves were fitted using the Gordon–Taylor equation (2). The Gordon–Taylor equation [14] can successfully describe the T_g behavior for miscible blends exhibiting negative and positive deviation if k is treated as an adjustable parameter. The equation indicates that k increases with increasing strength of the polymer interactions. Therefore, it does represent a qualitative measurement of interactions for comparison purposes, as demonstrated by several studies of miscible binary polymer blends [15].

A good fit was obtained using $k = 0.05$ for DO3/PS, $k = 0.111$ for DO3/PMMA and $T_{gDO3} = 325.2$ K. The values

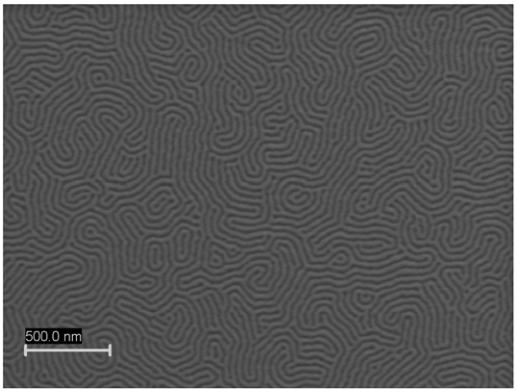

Figure 6. SEM morphology of PS-*b*-PMMA thin film.

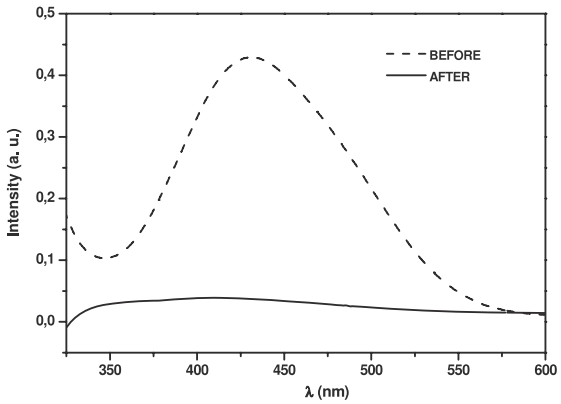

Figure 7. UV–vis spectra of 10 wt% DO3/PS-*b*-PMMA films before and after thermal annealing.

obtained for k parameters indicate a weaker interaction of DO3 with PS than with PMMA:

$$T_{g_{blend}} = \frac{w_{DO3}T_{g_{DO3}} + k(1 - w_{DO3})T_{g_{polymer}}}{w_{DO3} + k(1 - w_{DO3})}. \quad (2)$$

From the comparison of the solubility limits of both binary systems 10 wt% of DO3 could be dissolved in PMMA leading to a homogeneous solution in contrast to only 2 wt% in PS; in consequence the preferential affinity of DO3 for PMMA is demonstrated. Taking this into account, blends of DO3 in PS-*b*-PMMA in which DO3 was expected to locate into PMMA domains during PS-*b*-PMMA self-assembly were prepared. The self-assembly process was promoted by thermal annealing, which also had the aim of supporting the preferential location of the modifier in PMMA block via softening the material, and consequently favoring DO3 diffusion.

The selected PS-*b*-PMMA was an asymmetric DBC that self-assembled in hexagonal arrangements of ≈18 nm-diameter cylindrical PMMA domains (natural domain period $L_0 \approx 36$ nm) in a matrix of PS. Well-reproducible morphologies of the neat DBC were obtained using thermal annealing at 190 °C for 1 h to promote self-assembly [16]. We should mention that equilibrated morphologies were obtained after 1 h at 190 °C, since longer times did not produce any changes in the developed morphologies, in agreement with previous reported works [17–19]. A high temperature process allows us to dramatically reduce the annealing time [17, 20], providing an industrially appealing approach for the technological implementation of BC-based manufacturing protocols.

On bare silicon wafers, pure PS-*b*-PMMA thin films developed parallel oriented cylinders as expected for preferential surfaces (figure 6). Samples could be clearly analyzed without removing PMMA since the SEM electron beam damages and partially removes PMMA domains generating enough contrast in the SEM images. Darker gray regions correspond to PMMA and bright ones to PS.

Films of PS-*b*-PMMA containing different amounts of DO3 were prepared. Even though films displayed an intense orange color after spin-coating, they were colorless after thermal annealing. UV–vis spectra of a film of 10 wt% DO3/PS-*b*-PMMA showed the disappearance of the characteristic band of the DO3 at 440 nm after thermal annealing (figure 7). As DO3 was a free molecule dispersed in a thermoplastic matrix, migration of DO3 onto the free surface of the DBC occurred during thermal annealing, attributed to surface tension lowering [21]. The disappearance of color is due to the evaporation of the migrated DO3, since the melting temperature of DO3 is 200 °C (very close to the annealing temperature).

To avoid surface segregation of DO3, a thermoplastic polymer was synthesized (Azo-TP) from the bulk reaction of DO3 and DGEBA. The choice of DGEBA as the co-reactant was an attempt to encourage the selective location of azo groups in the PMMA phase of PS-*b*-PMMA. The selection was based on a previous work where homogeneous binary solutions of DGEBA with PMMA could be obtained in the whole composition range depending on the chain extender used [22]. In addition, it is well known that the solubility of PS in DGEBA is lower than the solubility of PMMA, which is very desirable in terms of preferential segregation of Azo-TP to the PMMA phase [23].

The Azo-TP was synthesized in a DO3/DGEBA ratio equal to 0.5. The polymerization was carried on at 180 °C. The reaction was stopped after 1 h to avoid polyetherification of epoxy that takes place at longer reaction times. Polyetherification leads to an azo-network which is undesirable in terms of film generation since it would result impossible to dissolve in the DBC. As epoxy was in excess respect to DO3, a considerable amount of unreacted epoxy groups remain in the final polymer. The idea of using a high excess of epoxy is to favor the miscibility of the Azo-TP in PMMA. The final conversion of epoxy groups was 0.38 as determined by FTIR. The resulting material exhibited an intense orange color and was completely amorphous with a T_g of 41 °C. The Azo-TP was characterized in terms of its optical activity (figure 8).

A good optical response was obtained in this case—a high Δn_{max} and an acceptable remnant birefringence (63%)—which may be attributed to the covalent bonding of azo molecules to the polymer chains. These good optical characteristics are expected to persist when Azo-TP is

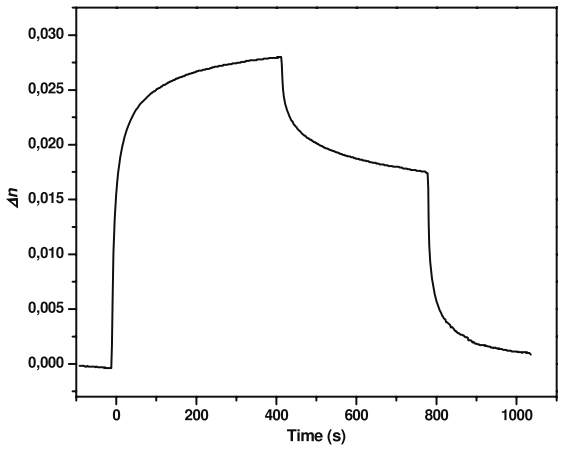

Figure 8. Writing and relaxation curve of an Azo-TP film.

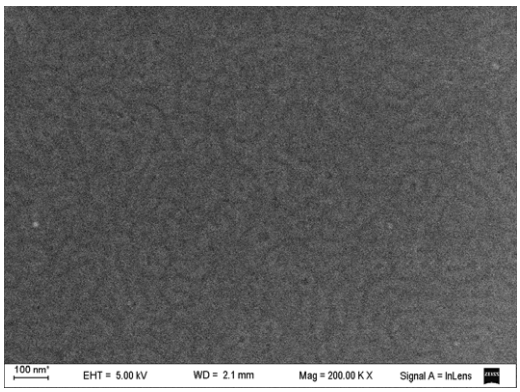

Figure 10. SEM image of a PS-*b*-PMMA film containing 12 wt% Azo-TP.

dispersed in the BC. In fact, they are expected to be enhanced by a confinement effect.

A preliminary inspection of solutions of Azo-TP in PS and PMMA homopolymers corroborates the preferential affinity of the Azo-TP for PMMA. Films containing 1–40 wt% of Azo-TP were prepared by solvent casting THF solutions onto glass slides and examined by TOM. Azo-TP/PMMA blends showed complete miscibility up to 30 wt% of Azo-TP at room temperature; instead Azo-TP/PS blends containing more than 1 wt% of Azo-TP were phase separated, figure 9.

PS-*b*-PMMA films of approximately 300 nm containing 12 wt% of Azo-TP (corresponding to 30 wt% with respect to the PMMA block of the DBC) were prepared by spin-coating. Perfect homogeneous orange films were obtained after thermal annealing, indicating the absence of migration of Azo-TP to the free surface. A SEM image of a film approximately 100 nm-thick spin-coated onto a Si wafer is displayed in figure 10. The presence of Azo-TP seems to hinder the process of nanostructuration, generating morphologies where the cylinders of PMMA could not be perfectly arranged. However, the remarkable aspect is that no macrophase separation or aggregation were observed, indicating that the Azo-TP could be mixed in the PMMA phase of the DBC.

Birefringence Δn measurements have been performed in as-prepared and annealed films of DBC containing 12 wt% Azo-TP in order to evaluate the effect of nanostructuration on optical response. The time evolution of Δn under a complete cycle of irradiation/switched off/circularly polarized light is shown in figure 11. When as-prepared, the film shows a comparable behavior to that obtained in the neat Azo-TP. Meanwhile, when annealed, it shows a slightly lower maximum birefringence but an increased remnant birefringence, probably due to the effect of confinement exerted by the PS phase. We also noted that in the annealed films the writing–relaxation curves are stable and reproducible (see figure 12). The measurements were repeated for samples that were stored under ambient conditions for at least 3 weeks, and essentially no changes in the photo-orientation dynamics, absolute birefringence or relaxation behavior could be observed.

To make an easy qualitative comparison of the evolution of Δn with irradiation time in the different polymers under study, we show in figure 13 Δn values normalized to its maximum value, Δn_{max}. All three polymer systems seem to exhibit quite similar behavior in terms of photoinduced time response. However, looking at the inset (which is a

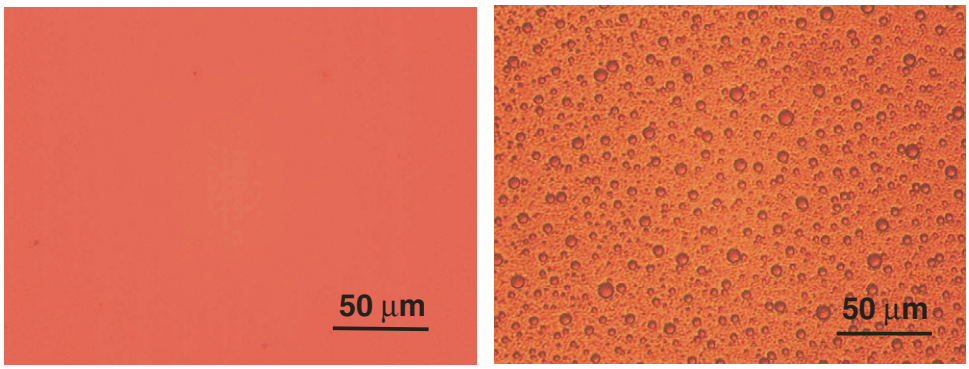

(a) (b)

Figure 9. (a) PMMA film containing 30 wt% of Azo-TP. (b) PS film containing 5 wt% of Azo-TP.

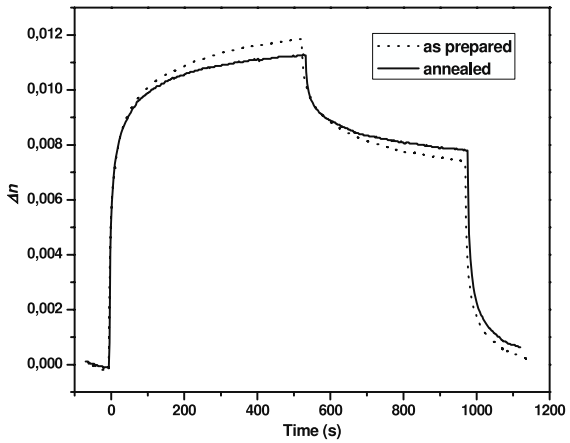

Figure 11. Writing and erasing curve for a PS-*b*-PMMA film containing 12 wt% Azo-TP before and after thermal annealing.

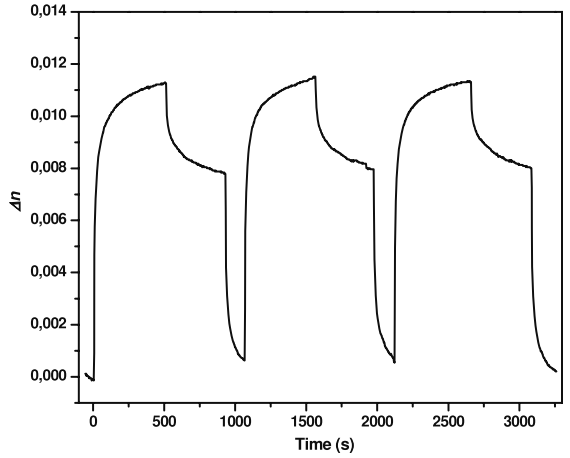

Figure 12. Repeated writing and erasing cycles for annealed PS-*b*-PMMA film containing 12 wt% Azo-TP.

Table 1. DO3 wt%, Δn_{max} and remnant birefringence of the different samples under study.

	DO3 (wt%)	Δn_{max}	Remnant birefringence
10 wt% DO3/PMMA	10	0.0155	42.4
20 wt% DO3/PMMA	20	0.0164	35.6
Azo-TP	25	0.0365	63.4
12 wt% Azo-TP/PS-*b*-PMMA (annealed)	3.4	0.0109	71.4

magnification of the writing process), the DO3 guest–host system shows a faster writing speed as expected due to the higher mobility of the chromophore in this system. The other two systems show comparable growing slope, meaning that the time response of the neat Azo-TP was preserved when it was dispersed in the DBC, which is very desirable in terms of the writing speed. Besides, there is a favorable confinement effect that produces an increment of the remnant anisotropy, probably due to a restriction in the azo mobility caused by interactions with the walls of the nanodomains that slow down the randomization of azo molecules. The improvement in

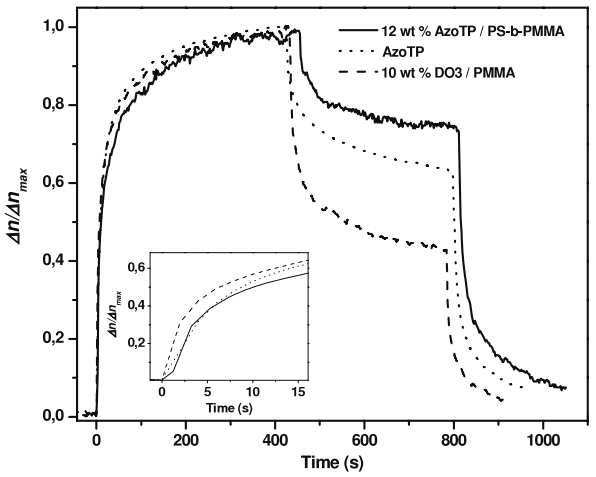

Figure 13. Evolution of Δn normalized to its maximum value Δn_{max} versus time. Inset: magnification of the first seconds of irradiation.

remnant anisotropy is very important since it is the major requirement in optical storage applications.

Table 1 shows the values of Δn_{max} and remnant birefringence of the different samples under study as a function of DO3 wt%. The maximum induced birefringence is only a function of the overall chromophore concentration for Azo-TP containing materials. The level of maximum birefringence in Azo-TP was 0.0365 (for 25 wt% DO3), while that measured for the DBC containing Azo-TP was 0.0109 (for 3.4 wt% DO3). These values are similar to previously published systems, such as the studies of the photo-orientation in epoxy [24] and melamine [25] networks containing DO3. Normalizing to DO3 concentration, the guest–host system based on the DBC showed the higher value of maximum photoinduced birefringence.

4. Conclusions

We tried to use the asymmetric diblock copolymer PS-*b*-PMMA as a host for DO3 in order to develop photoinduced optical birefringence in its thin films. However, it was necessary to synthesize a DO3-based thermoplastic (Azo-TP) to avoid DO3 to migrate during thermally promoted block copolymer self-assembly. The Azo-TP could be satisfactorily dissolved in the PS-*b*-PMMA since no macrophase separation or aggregation was observed. The resulting material showed the higher value of photoinduced birefringence when compared with the simple guest–host system or the Azo-TP (normalized to DO3 concentration). In terms of remnant anisotropy, there is a notable improvement caused by the confinement exerted by the DBC. So, this makes them promising materials for use in optical storage applications.

Acknowledgments

The financial support of the University of Mar del Plata, the National Research Council (CONICET) and the National

Agency for the Promotion of Science and Technology (ANPCyT) is gratefully acknowledged.

References

[1] Lee K M, Koerner H, Vaia R A, Bunning T J and White T J 2010 *Macromolecules* **43** 8185
[2] Dumont M and El Osman A 1999 *Chem. Phys.* **245** 437
[3] Natansohn A and Rochon P 2002 *Chem. Rev.* **102** 4139
[4] Barto R R *et al* 2006 *Macromolecules* **39** 7566
[5] Lagugne-Labarthet F, Buffeteau T and Sourisseau C J 1998 *Phys. Chem.* B **102** 2654
[6] Lachut B L, Maier S A, Atwater H A, de Dood M J A, Polman A, Hagen R and Kostromine S 2004 *Adv. Mater.* **16** 1746
[7] Fukuda T, Kim J Y, Barada D and Yase K J 2006 *Photochem. Photobiol.* A **182** 262
[8] Okano K, Shishido A and Ikeda T 2006 *Adv. Mater.* **18** 523
[9] Yu H, Kobayashi T and Yang H 2011 *Adv. Mater.* **23** 3337
[10] Yu H, Shishido A, Iyoda T and Ikeda T 2007 *Macromol. Rapid Commun.* **28** 927
[11] Forcén P, Oriol L, Sánchez C, Alcalá R, Hvilsted S, Jankova K and Loos J 2007 *J. Polym. Sci.* A **45** 1899
[12] Tian Y, Watanabe K, Kong X, Abe J and Iyoda T 2002 *Macromolecules* **35** 3739
[13] Fernández R, Mondragon I, Oyanguren P A and Galante M J 2008 *React. Funct. Polym.* **68** 70
[14] Gordon M and Taylor J 1952 *J. Appl. Chem.* **2** 493
[15] Lu X and Weiss R A 1992 *Macromolecules* **25** 3242
[16] Zucchi I A, Poliani E and Perego M 2010 *Nanotechnology* **21** 185304
[17] Guarini K W, Black C T and Yeung S H I 2002 *Adv. Mater.* **14** 1290
[18] Han E, Stuen K O, Leolukman M, Liu C-C, Nealey P F and Gopalan P 2009 *Macromolecules* **42** 4896
[19] Chen S-C, Kuo S-W, Jeng U-S, Su C-J and Chang F-C 2010 *Macromolecules* **43** 1083
[20] Zhang X, Berry B C, Yager K G, Kim S, Jones R L, Satija S, Pickel D L, Douglas J F and Karim A 2008 *ACS Nano* **2** 2331
[21] Fernández R, Zalakain I, Ramos J A, Martin L and Mondragon I 2011 *Eur. Polym. J.* **47** 1176
[22] Ritzenthaler S, Girard-Reydet E and Pascault J P 2000 *Polymer* **41** 6375
[23] Zucchi I A, Galante M J and Williams R J J 2005 *Polymer* **46** 2603
[24] Fernandez R, Mondragón I, Galante M and Oyanguren P 2009 *J. Polym. Sci.* B **47** 1004
[25] Takase H, Natansohn A and Rochon P 2001 *J. Polym. Sci.* B **39** 1686